$Ln_{13}Br_{18}B_3$ (Ln = Gd, Tb)—A Compound Containing a Combination of Discrete and Condensed Clusters**

Oliver Oeckler, Lorenz Kienle, Hansjürgen Mattausch, and Arndt Simon*

Dedicated to Professor Dieter Fenske on the occasion of his 60th birthday

Metal-rich ternary halides of rare-earth metals form a large group of compounds,[1] the diverse structures of which can be understood within the concept of condensed clusters.[2a] As a rule, the cluster units of the valence-electron-poor rare-earth metals need stabilization by interstitial (endohedral) atoms.[2b] While several types of clusters are observed, octahedral units of metal atoms condensed through edges dominate. The structural systematics range from compounds with discrete clusters to those with chains and layers to those with three-dimensional (3D) networks, as illustrated with some arbitrary examples of the particularly rich chemistry of boride and carbide halides.[3]

The structure of $Tb_7X_{12}B$ (X = halogen) contains discrete Tb_6BX_{12} clusters.[1c] The compound $Tb_{10}Br_{15}B_2$, which contains a $Tb_{10}B_2X_{18}$-type cluster built from two octahedral units fused through a common edge,[3a] represents the first condensation step towards the formation of infinite chains as in Tb_4X_5B.[3b] Four Tb_6B octahedra are linked to form discrete clusters with a $Tb_{16}B_4$ core in $Tb_{16}Br_{23}B_4$,[3c] and this cluster type is the building block of double chains as found in the carbide halide $Gd_6Br_7C_2$.[3d] Fusing an infinite number of chains results in a layer as, for example, in Gd_2X_2C.[3e] Last but not least, a 3D network is present in the structure of Gd_3X_3B.[3f,g]

Here we report on the structure of a reduced rare-earth metal halide that is the first to contain both discrete clusters and chains. This combination is found in the compounds $Ln_{13}Br_{18}B_3$ (Ln = Gd, Tb), which can be prepared from mixtures of $LnBr_3$, Ln, and B at approximately 1000 °C[4] and which form pillar-shaped, dark golden crystals.

X-ray diffraction patterns of single crystals of these compounds are characterized by sharp Bragg reflections besides pronounced diffuse scattering arranged in the form of rods along the c^* direction (Figure 1a). This indicates a disordered stacking of ordered layers. The average structure of the compound was solved on the basis of the intensities of Bragg reflections only, and the refinement converged to R values below 0.03. It is described in the orthorhombic space group *Immm*.[5] Figure 2a depicts the structure of $Ln_{13}Br_{18}B_3$ in a projection along [100]; the disorder is not obvious because it only affects the site occupation factors of some of the atoms. The structure consists of a honeycomb packing of well-ordered, single chains of *trans* edge-sharing Ln_6 octahedra, which are centered by B atoms and surrounded by Br atoms (Figure 2b). The channels between these single chains are filled by double chains (Figure 2a). In spite of the very convincing agreement between observed and calculated Bragg intensities, the average structure does not allow a reasonable chemical interpretation as some of the atomic positions are partially occupied as mentioned above and/or characterized by highly anisotropic displacement parameters.

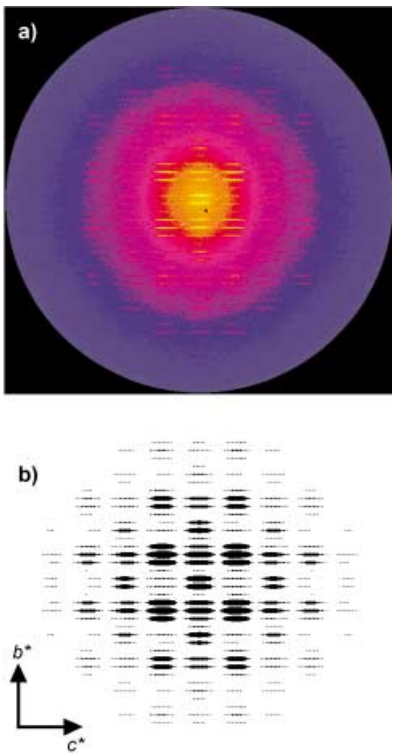

Figure 1. X-ray diffraction patterns of the 0.5*kl* section of reciprocal space: a) experiment (calculated from a series of imaging plate exposures); b) simulated on the basis of a $2 \times 2 \times 2$ supercell model, which approximates statistical disorder of the ordered layers.

The disorder problem could be solved by means of high-resolution transmission electron microscopy (HRTEM).[6] A HRTEM image taken along the [110] zone axis (Figure 3) clearly shows the nature of the disorder. First, the double chain resolves into a regular stacking of $Ln_{10}B_2$ units formed by edge-sharing Ln_6B octahedra and surrounded by Br atoms (Figure 2c). The image simulation image based on this model is in good agreement with the observed image (cf. the inset in Figure 3). Second, the stacks of well-ordered clusters are shifted relative to each other in an irregular way. This statistical arrangement is the origin of the diffuse scattering shown in Figure 1. A calculated diffraction pattern based on perfectly ordered clusters within layers parallel (001) and assuming stochastic disorder along [001] in the stacking of such layers in a suitable supercell mimics the intensity distribution of the diffuse scattering very well (Figure 1b).

The real structure of $Ln_{13}Br_{18}B_3$ (Ln = Gd, Tb) corresponds to the earlier mentioned honeycomb packing of single chains of condensed Ln_6B units surrounded by Br as in the M_6X_{12} cluster. The composition of one chain is Ln_4BBr_6. Owing to linkage through i–i contacts, that is contacts between anions of

[*] Prof. Dr. A. Simon, Dr. O. Oeckler, Dr. L. Kienle, Dr. H. Mattausch
Max-Planck-Institut für Festkörperforschung
Heisenbergstrasse 1, 70569 Stuttgart (Germany)
Fax: (+49) 711-689-1091
E-mail: a.simon@fkf.mpg.de

[**] We thank V. Duppel for recording high-resolution transmission electron microscopy images and electron diffraction patterns and R. Eger for the preparation of numerous samples.

  0044-8249/02/4122-4257 $ 20.00+.50/0

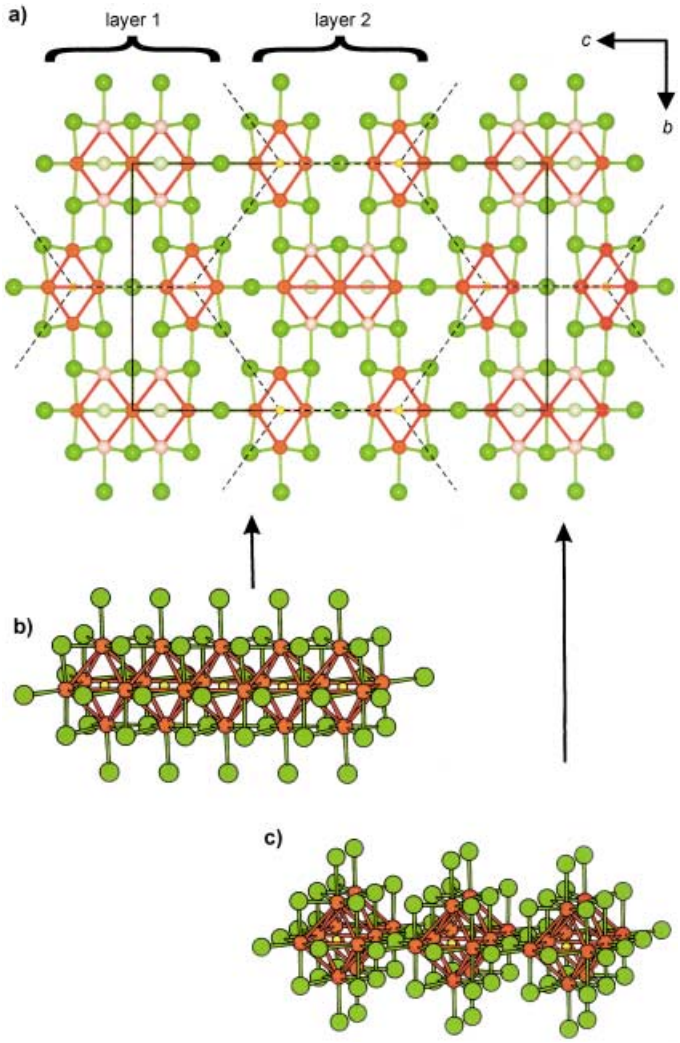

Figure 2. Crystal structure of $Ln_{13}Br_{18}B_3$ (Ln: red, Br: green, B: yellow): a) projection along [100] (the unit cell and layerlike structure are indicated, the honeycomb arrangement of single chains is highlighted by broken lines), Ln positions that are partially (50%) occupied in the average structure are depicted in pale red, pale green symbolizes a 1:1 mixture of Br and B; b) single chains of Ln_6B octahedra surrounded by Br atoms; c) regular stacking of $Ln_{10}B_2$ units along [100] within the ordered layers (appears as a double chain with partially occupied positions in the average structure).

the inner sphere, the substructure of the chains can be described as $Ln_{16}B_4Br_{18}Br^{i-i}_{6/2}$ in the notation of Schäfer and Schnering.[7] The channels are filled with $Ln_{10}B_2Br_{18}$ clusters. The Br atoms only partially belong to one cluster according to the formula $Ln_{10}B_2Br_{12}Br^{i-i}_{6/2}$. The chains and the clusters add up to the compound composition $Ln_{26}B_6Br_{36} = Ln_{13}Br_{18}B_3$. According to the Zintl–Klemm concept, the formal charge balance corresponds to the formula $Ln^{3+}{}_{13}Br^{-}{}_{18}B^{5-}{}_{3}e^{-}{}_{6}$. The excess of electrons leads to metallic properties as verified by conductivity measurements.

In addition to the i–i type bonds, in which Br atoms coordinate only edges of the Ln_6 octahedra, there are also i–a type connections that involve both an edge and a corner of neighboring octahedra. Figure 2a shows that the number of i–a type bonds is particularly large in layers parallel to (001), in fact, twice as many as i–i bonds in the orthogonal direction.

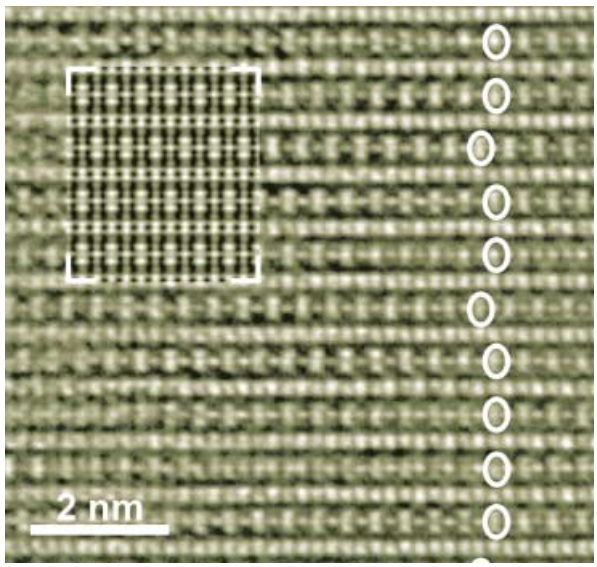

Figure 3. HRTEM image (zone axis [110]): the ellipsoidal marks highlight the positions of the disordered layers; inset: image simulation (defocus −45 nm, crystal thickness 3.5 nm) based on the $2\times2\times2$ supercell mentioned with Figure 1b.

This bond pattern yields an argument for both the perfect order in the layers and their statistical disorder.

The chain octahedra adopt positions around $x = 0, 1, 2, \ldots$ (layer 1) and $x = 1/2, 3/2, 5/2, \ldots$ (layer 2) in adjacent layers. The number of $Ln_{10}B_2$ double octahedra is half that of chain octahedra, hence the double octahedra lie either in $x = 1/2, 5/2, 9/2, \ldots$ or $x = 3/2, 7/2, 11/2, \ldots$ in layer 1 and either in $x = 0, 2, 4, \ldots$ or $x = 1, 3, 5, \ldots$ in layer 2. Electrostatic repulsion maximizes the distances between clusters and leads to a strict alternation of $x = 1/2, 5/2, 9/2, \ldots$ and $x = 3/2, 7/2, 11/2, \ldots$, respectively, for neighboring rows of double octahedra within the strongly interconnected layer 1, that is along [010]. With respect to the restriction for layer 1, there is no energetic difference between the alternatives $x = 0, 2, 4, \ldots$ and $x = 1, 3, 5, \ldots$, for the positioning of the clusters in layer 2. The origin of the resulting disorder is therefore due to a type of frustration, which is reminiscent of the fundamental phenomenon of frustrated antiferromagnetism in a triangular Ising net.[8] The interaction between disordered clusters belonging to neighboring layers is identical. The same situation would hold for the magnetic moments in a distorted orthohexagonal Ising net, in which the axial ratio is larger than $\sqrt{3}$ and where the interaction within a layer is stronger than between layers.

Received: May 31, 2002
Revised: August 15, 2002 [Z19420]

[1] a) J. D. Corbett, *J. Chem. Soc. Dalton Trans.* **1996**, 575–585; b) G. Meyer, *Chem. Rev.* **1988**, *88*, 93–107; c) A. Simon, H. Mattausch, G. J. Miller, W. Bauhofer, R. K. Kremer, *Handbook on the Physics and Chemistry of Rare Earths, Vol. 15* (Eds.: K. A. Gschneidner, Jr., L. Eyring), North Holland, Amsterdam, **1991**, pp. 191–285.
[2] a) A. Simon, *Angew. Chem.* **1981**, *93*, 23–44; *Angew. Chem. Int. Ed. Engl.* **1981**, *20*, 1–22; b) A. Simon, *Angew. Chem.* **1988**, *100*, 163–188; *Angew. Chem. Int. Ed. Engl.* **1988**, *27*, 159–183.
[3] a) H. Mattausch, E. Warkentin, O. Oeckler, A. Simon, *Z. Anorg. Allg. Chem.* **2000**, *626*, 2117–2124; b) H. Mattausch, O. Oeckler, A. Simon, *Inorg. Chim. Acta* **1999**, *289*, 174–190; c) H. Mattausch, G. V. Vajenine,

  0044-8249/02/4122-4258 $ 20.00+.50/0

O. Oeckler, R. K. Kremer, A. Simon, *Z. Anorg. Allg. Chem.* **2001**, *627*, 2542 – 2546; d) U. Schwanitz-Schüller, Ph.D. thesis, Stuttgart, **1984**; e) U. Schwanitz-Schüller, A. Simon, *Z. Naturforsch. B* **1985**, *40*, 710 – 716; f) E. Warkentin, A. Simon, *Rev. Chim. Miner.* **1983**, *20*, 488 – 495; g) C. Zheng, O. Oeckler, Hj. Mattausch, A. Simon, *Z. Anorg. Allg. Chem.* **2001**, *627*, 2151 – 2162.

[4] For the synthesis of $Tb_{13}Br_{18}B_3$ [$Gd_{13}Br_{18}B_3$], Ta capsules were filled with $TbBr_3$ (1000 mg) [$GdBr_3$ (750 mg)], Tb (433 mg) [Gd (323 mg)] and B (14.4 [10.7] mg; 5N, Aldrich) and sealed under Ar by arc-melting. These were heated for 30 days at 950 °C [6 days at 1000 °C]. Further details are analogous to the procedures described in reference [3g]. The compounds can be obtained as almost single-phase products according to X-ray powder diagrams. They are sensitive to moisture and need to be handled in a dry inert gas atmosphere.

[5] Single-crystal X-ray investigation (average structure): Stoe IPDS diffractometer, $Mo_{K\alpha}$ (0.71073 Å), $2\theta_{max} = 60.6°$; orthorhombic, space group *Immm*; $a = 3.9923(2)$, $b = 17.0462(12)$, $c = 28.3039(19)$ Å for $Gd_{13}Br_{18}B_3$ and $a = 3.9637(3)$, $b = 16.9063(13)$, $c = 28.1068(18)$ Å for $Tb_{13}Br_{18}B_3$; least-squares refinement on F^2 (G. M. Sheldrick, SHELXL 97 program for the refinement of crystal structures, University of Göttingen, Göttingen (Germany), **1997**); R_1 [$I \geq 2\sigma(I)$] = 0.025 (0.022), wR_2 [all data] = 0.057 (0.046) for 1668 (1627) reflections and 76 (76) parameters for $Gd_{13}Br_{18}B_3$ ($Tb_{13}Br_{18}B_3$). Further details on the crystal structure investigation may be obtained from the Fachinformationszentrum Karlsruhe, 76344 Eggenstein-Leopoldshafen, Germany (fax: (+49) 7247-808-666; e-mail: crysdata@fiz-karlsruhe.de), on quoting the depository numbers CSD-412541 ($Gd_{13}Br_{18}B_3$) and CSD-412540 ($Tb_{13}Br_{18}B_3$). A detailed description of the structural analysis as well as an analysis of symmetry relationships and additional real structure phenomena will be published elsewhere (O. Oeckler, L. Kienle, H. Mattausch, O. Jarchow, A. Simon, *Z. Kristallogr.*, submitted).

[6] HRTEM images were recorded with a Philips CM30 ST electron microscope (300 kV, LaB_6 cathode, Gatan multiscan CCD camera). The multislice formalism (P. A. Stadelmann, *Ultramicroscopy* **1987**, *21*, 131 – 146) was used for image simulations.

[7] H. Schäfer, H. G. Schnering, *Angew. Chem.* **1964**, *76*, 833 – 849.

[8] G. H. Wannier, *Phys. Rev.* **1950**, *79*, 357 – 364.

Enzymatic Elongation of the LEC14 Antigen Generates a β-1,2 Arm on *N*-Glycans**

Ingo Prahl and Carlo Unverzagt*

This work is dedicated to Professor Hans Paulsen on the occasion of his 80th birthday

Nearly all proteins of the blood serum and on cell surfaces in higher organisms are glycosylated.[1,2] On these glycoproteins, a multitude of asparagine-linked oligosaccharides (*N*-glycans) with similar structures are found. The structural diversity of these *N*-glycans is generated biosynthetically from a common core pentasaccharide $Man_3GlcNAc_2$. In biologically relevant complex *N*-glycans, this core pentasaccharide is extended by up to five antennae and can be modified further by the addition of single sugar residues, for example, core fucose or a bisecting GlcNAc residue. Recently, mutants of Chinese hamster ovary cells (CHO cells) termed LEC14 were found to exhibit *N*-glycans with a new glycosylation motif at the core pentasaccharide.[3] The structural analysis indicated an additional GlcNAc residue β-1,2 linked to the β-mannoside of the core trisaccharide. The relevant glycosyltransferase was characterized and termed GlcNAc-TVII.[4] To confirm the proposed structure and generate derivatives for biological evaluation, we have synthesized the LEC14 nonasaccharide, functionalized with a spacer. Analysis of the NMR spectroscopic data indicates that the proposed structure is correct. Unexpectedly, the single GlcNAc residue present in the LEC14 motif of the synthetic target compound was recognized by galactosyltransferase, which resulted in a to date unknown type of branching extension. The occurrence of this novel antenna (β-1,2 arm) generates a third branch at the central β-mannoside. This arm adds a new element to the structural motifs of *N*-glycan cores, which permits even greater variability.

A protected form of the LEC14 nonasaccharide **1** was obtained by using a modular building-block approach[5] based on regio- and stereoselective glycosylations.[6] The synthesis of the LEC14 *N*-glycan was designed to allow a comparison with the isolated natural compound and to give access to neoglycoconjugates for future investigation of the biological activity of this unusual *N*-glycan.[7] Furthermore, the synthetic LEC14 *N*-glycan should be elongated using glycosyltransferases to give full length *N*-glycans with biologically relevant termini.

The conversion of the protected nonasaccharide **1** into neoglycoconjugates required several synthetic steps, which included the coupling of the carbohydrate moiety to a spacer that can be selectively activated for later attachment to the carrier.[8] Prior to the coupling of the spacer, all protecting groups except the three benzyl groups and the anomeric azido group were removed sequentially.

First, the three *p*-methoxybenzyl groups (Mpm) of the fucose residue in compound **1** were oxidatively removed using ceric ammonium nitrate (CAN) in acetonitrile/water. The phthaloyl groups of the nonasaccharide **2** were removed in a one-pot reaction comprising three steps, which was developed for use with *N*-glycans without affecting anomeric azido groups. Using ethylene diamine in *n*-butanol[9] at 80 °C yielded an intermediate pentaamino compound. After acetylation and *O*-deacetylation, the water-soluble nonasaccharide **3** was isolated by solid-phase extraction (SPE) in 96 % overall yield. Subsequent reduction of the azido group using excess propanedithiol in methanol/triethylamine[10] yielded the corresponding glycosylamine after removal of the volatile reagents. The amine was immediately acylated with excess *N*-benzyloxycarbonyl-6-aminohexanoic acid **4** using *O*-(benzotriazol-1-yl)-1,1,3,3-tetramethyluronium tetrafluoroborate/hydroxybenzotriazole (TBTU/HOBt) in *N*-methyl-2-pyrrolidone (NMP). Under these conditions, *O*-acylation was observed, which could be reversed by quenching the reaction mixture with aqueous methylamine prior to workup. After purification by reverse-phase (RP)-HPLC, **5** was obtained in 31 % yield. Catalytic hydrogenation over palladium hydroxide furnished the aminohexanoyl-derivatized nonasaccharide **6** in 95 % yield after size-exclusion chromatography (Scheme 1).

[*] Prof. C. Unverzagt, I. Prahl
Bioorganische Chemie, Gebäude NW1
Universität Bayreuth, 95440 Bayreuth (Germany)
Fax: (+49) 921-555365
E-mail: carlo.unverzagt@uni-bayreuth.de

[**] We thank the Deutsche Forschungsgemeinschaft and the Fonds der Deutschen Chemischen Industrie as well as Aventis Research and Technology for funding. Gratitude is expressed to Roche Diagnostics for supplying reagents.

  0044-8249/02/4122-4259 $ 20.00+.50/0